PNOC 96

THE NATURAL STATE MODEL OF THE RESERVOIR OF THE MINDANAO I GEOTHERMAL FIELD

Miguel B. Esberto

PNOC Energy Development Corp., Memtt Road, Fort Bonifacio, Makati City, Philippines

Abstract

The Mindanao I Geothermal Field is a typical andesitic volcano-hosted hydrothermal system in a high relief topography. The conceptual model of the field suggests that the upwelling fluids are beneath the Sandawa Collapse northwest of the Mt. Apo peak A reservoir of two-phase fluids exists above -250 to 0 m RSL from where boiling is postulated to occur. The outflowing fluids move towards the northwest through the various structures in the Marbel Corridor. They are diverted to the north by the cold Matingao Block before being discharged to the surface through the chloride springs of Imba, Marbel and Sisiman.

A three-dimensional natural state model of the reservoir was developed using the MULKOM computer code. The steady state model was calibrated against the field data. The best fit natural state closely corresponds to the conceptual model of the field. The model suggests that the convective system of the reservoir has a natural recharge of 70 kg/s with an enthalpy of 1600 kJ/kg.

1 INTRODUCTION

The Mindanao 1 Geothermal Field (M1GF) is situated in the southwestern part of the island of Mindanao, Philippines which is within the Mt. Apo Geothermal *Area* (Figure 1). Geoscientific exploration in the Mt. Apo area identified several potential sites, the most promising prospect among them is the *Marbel Anomaly* northwest of the Mt. Apo peak. Following the discovery of a high temperature resource in this sector, two deep exploratory wells were drilled and subsequently tested in 1987 and 1988.

Development of the field commenced in 1992 with a 701-hectare area (Mindanao 1 Geothermal Project or MIGP) segregated from the *52,262* hectare Mt. Apo National Park to be targeted for geothermal exploitation. To date, 25 wells have *already* been completed Of these, 9 wells will be tapped for production for the first *52* MWe power plant.

A simulation *study* was made with the objective of developing a preliminary numerical model for the M1GF, specifically to generate the natural state of the reservoir. The simulation runs were made using the MULKOM computer code at the School of Engineering, University of Auckland, in Auckland, New Zealand

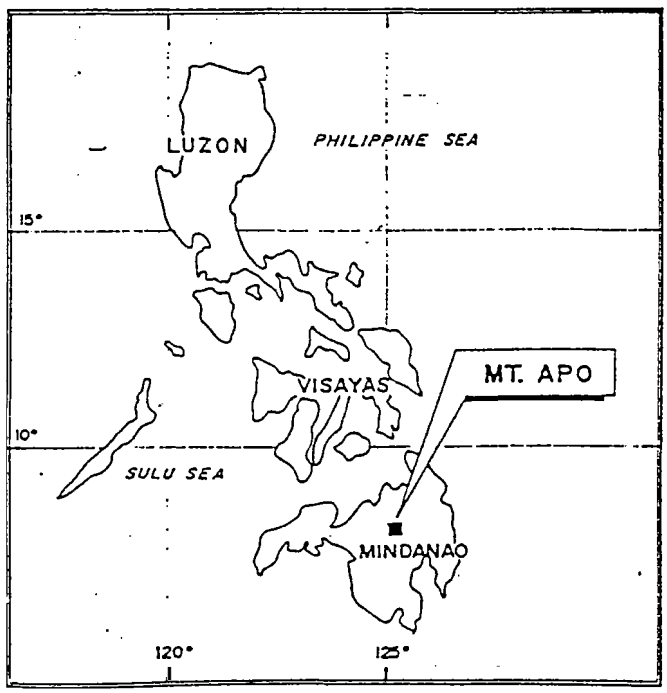

Figure 1. Location of Mt. Apo in the island of Mindanao where the M1GF is situated.

2 PREVIOUS STUDIES

Extensive drilling of deviated and vertical wells in MlGF produced valuable scientifc data resulting to a better understanding of the reservoir. This provided valuable insights for the development and future exploitation of the field The succeeding sections briefly discussed the geoscientific and reservoir engineering analysis of the undisturbed reservoir. Most of the discussions are referred from the 1994 Resource Assessment Update of the field

2.1 GEOLOGY OF THE FIELD

Geologic structures such as faults and their associated fracturing are believed to be the conduits for thermal fluids in MlGF with minor contributions coming from lithologic contacts. The field has three major structural features which influence the hydrogeological activity of the system.. These are (1) the *Sandawa Collapse,* a topographic depression situated in .the southeast sector of the field, (2) the *Marbel Corridor,* located northwest of Sandawa Collapse featured by the NW-SE trending Marbel Fault Zone, and (3) the Matingao Block, situated within the Matingao Collapse (Figure 2).

In the Matingao Block, where the reinjection wells are collared, the structures indicated good permeabilities. However, cold fluid invasions in structures are prevalent. In the Marbel Corridor, relatively hotter fluids are conveyed by'the northwest-southeast trending faults. The Marbel Fault Zone and the Sabpangon South faults are considered to be the most permeable within this block and within the field Fair to good permeabilities in these fault planes exist down to 0 m RSL. Deeper permeabilities vary from fair to poor. Structures intersected by wells within the Sandawa Collapse indicate fair permeabilities and are believed to be the conduits for the upwelling thermal fluids.

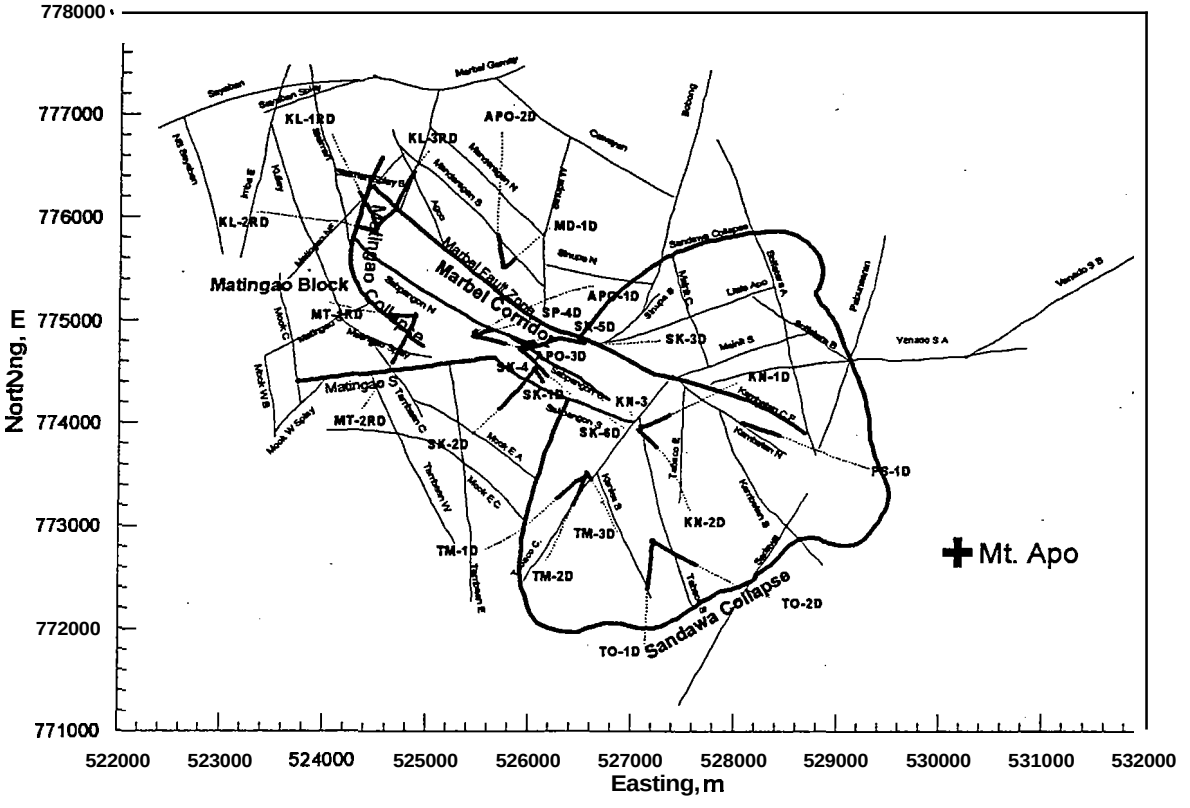

Figure 2. The structural and location map of wells in M1GF.

The subsurface geology of MIGF consists basically of andesitic lava flows, breccias and tuffs known as Apo Volcanics (*AV*). It is subdivided into an older (*oAV*) and a younger (*yAV*) member. The *yAV* is mostly confined to the peak of Mt. Apo. The *oAV* forms the dissected and eroded flanks of Mt. Apo. It is further subdivided into 2 subunits, an upper (*oAVu*) and a lower (*oAVl*) sequence, which are separated by a paleosol horizon. The *oAVu* is composed mainly of hornblende andesite, dacite. and tuff breccias. The lower *oAVl* is composed of basaltic andesite to basalt and tuff breccias. Underlying the *AV* is the Sabpangon Sedimentary Formation. This formation consists of carbonaceous sandstone, siltstone and rare limestone intercalated with hyaloclastite. The next rock unit are the completely metamorphosed volcanics which comprise the Contact Metamorphic Zone. Lastly, the Sandawa Intrusive, intersected in one well was composed of fresh biotite hornblende-quartz monzodiorite cut by andesitic/dacitic dikes.

2.2 GEOPHYSICAL STUDIES

The geophysical studies conducted identified several low resistivity areas in the Mt. Apo Geothermal *Area* (PNOC-EDC, 1989). The most promising among them is located in the northwestern flank of Mt. Apo volcano. This area, the ***Marbel Anomaly,*** is defined by the 100 ohm-m contour enclosing apparent resistivities of 10 - 50 ohm-m. The resistivity model defined a geophysical resource area of 15 to 30 km^2 and is bounded in the southeast by the rim of the Sandawa depression and to the northwest by the chloride springs of Imba, Marbel, and Sisiman.

2.3 CHEMISTRY OF THE FLUIDS

Typical for a strato-volcanic hydrothermal system, acid-SO_4 and HCO_3 springs are situated along the flanks of the volcano and the chloride springs several kilometres away (PNOC-EDC, 1989). Acid-SO_4 water exists in the Agco and Mainit (1500 m RSL) areas. A manifestation inside the cold acid-altered ground is the neutral pH *mixed* SO4 - HCO_3 spring of Pabunsaran (1780 m RSL). Chloride springs are present along the Imba Creek (840 m RSL), Marbel River (1025 m RSL) and Sisiman River (1100 m RSL), the highest so far recorded in any Philippine geothermal field These hot to boiling neutral pH springs contains between 1000-3000 ppm Cl.

The 1994 Resource Assessment Update identified three types of discharge fluids. These are (a) the neutral pH Na-CI liquids tapped by the wells spudded in the Matingao Block and the Marbel Corridor; (b) the neutral pH to slightly acidic Na-SO_4 condensed *steam* at 400-900 m RSL in the Marbel Corridor and the Sandawa Collapse, (c) the acid Na-Cl (+SO_4) liquid in the deeper parts of the Sandawa Collapse. Salonga (1995) classified a fourth type of fluid and it contains high concentrations of dissolved SO_4, HSO_4, low Cl and is postulated to be acid-condensate formed at the shallow levels of Mt. Apo which descends to intermediate depths.

The chloride concentration of deep reservoir waters in the upflow area exceeds 5000 mg/kg. Iso-chloride contours illustrate that Cl is highest inside the Sandawa Collapse. This declines as the fluids move towards the Marbel Corridor and the Matingao Block.

2.4 TEMPERATURE AND PRESSURE DISTRIBUTION

Figure 3 illustrates the temperature distribution at 0 m RSL. Interpretation suggests that the upwelling of hot thermal fluids occurs inside the Sandawa Collapse and within the vicinity of wells KN-ID, KN-2D, KN-3B and PS-ID. The outflow in the Marbel Corridor is towards the northwest. The fluid movement, however, deviates towards APO-2D upon encountering an impermeable column that separates the hot Marbel Corridor and the colder fluids in the Matingao sector.

Boiling inside the Sandawa Collapse *occurs* at approximately 0 m RSL and two-phase conditions exist above it. Wells that tap this zone are characterised by high discharge enthalpies. A vapour dominated zone exists above the two-phase fluids inside the Sandawa Collapse and at shallow depths in the outflow sector.

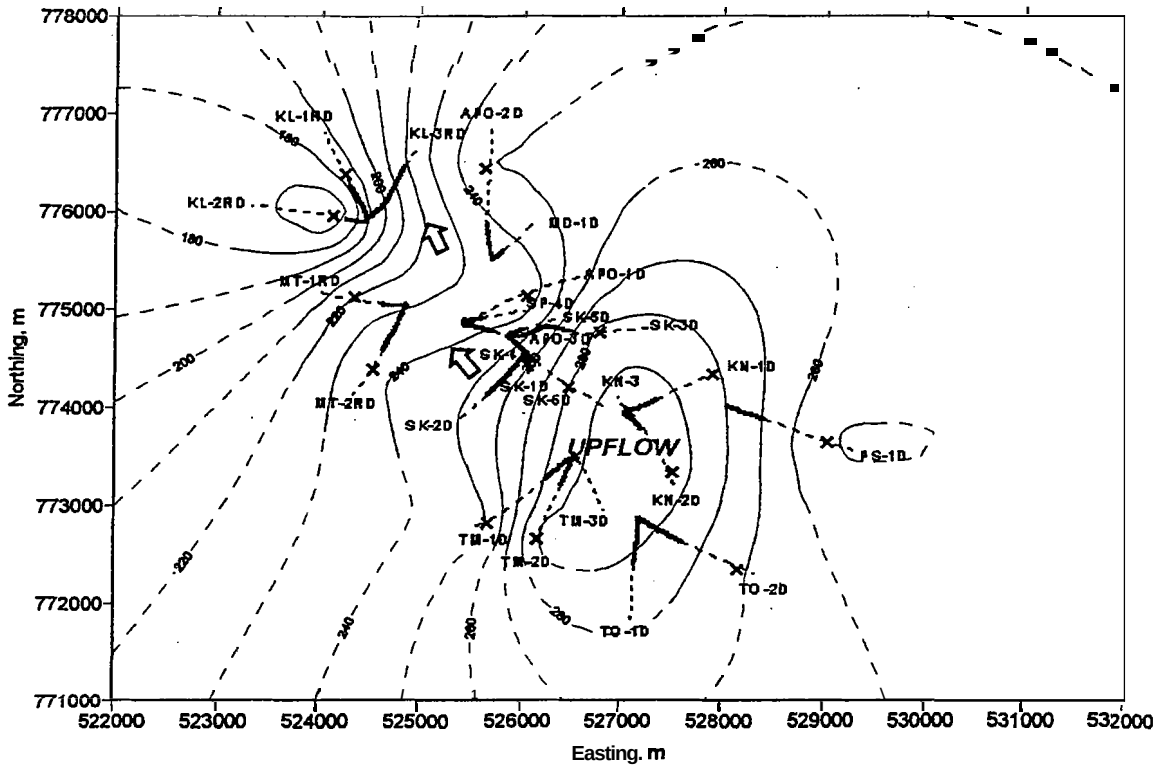

Figure 3. Temperature distribution in MGF reservoir at 0 m RSL (modified after **PNOC-EDC,** 1994).

The highest pressures were measured in wells KN-ID, KN-2D and **PS-ID** that lie above the upflow zone. **Pressures** in the cold **Matingao** Block are observed to **be** relatively higher **than** in the Marbel Corridor. These caused the **deviation** of the outflowing **fluids** towards the north resulting in hotter measured temperatures at shallow levels **in** wells **APO-2D** and MD-1D. The pressure contour lines at higher elevations are more closely packed **near** the **Matingao** Block suggesting the presence of an impermeable block between the Marbel Corridor and the Matingao Block

2.5 PERMEABILITY DISTRIBUTION AND PERMEABLE ZONES

The locations of the permeable zones were deduced from **drilling** logs, circulation losses, **geological** interpretations and **downhole** temperature measurements. The permeable zones in **MGF** are located within the range of 800 m RSL to 1300 m RSL and these **feed** zones are controlled **by** the structures that are intersected **by** the wells (Figure **4).**

Sector	Average Injectivity Index *l/s-MPa*	Average Transmissivity *darcy-meter*
Matingao Block		
Pad B	14.4	11.9
Pad RA	40.0	13.0
Pad RI	44.4	4.5
Marbel Corridor		
Pad A	260.7	95.0
Pad E_{upper}	87.6	-
Pad E_{lower}	48.3	19.4
Sandawa Collapse		
Pad C	22.0	2.8
Pad F	16.1	1.3
Pad G	37.0	1.6
Pad H	9.4	0.4

Table 1. Average injectivities and transmissivity on each sector.

The average injectivities and permeability-thickness product **on** each sector are tabulated in Table 1. Injectivity and pressure transient test results **obtained during** completion tests show that the permeability increases **from** the Sandawa Collapse towards the Marbel Corridor and the Matingao **Block** The relatively **high** permeability

shown by wells in the Marbel Corridor correlates with the fact that it is the major flowpath of the upwelling fluids from the Sandawa Collapse.

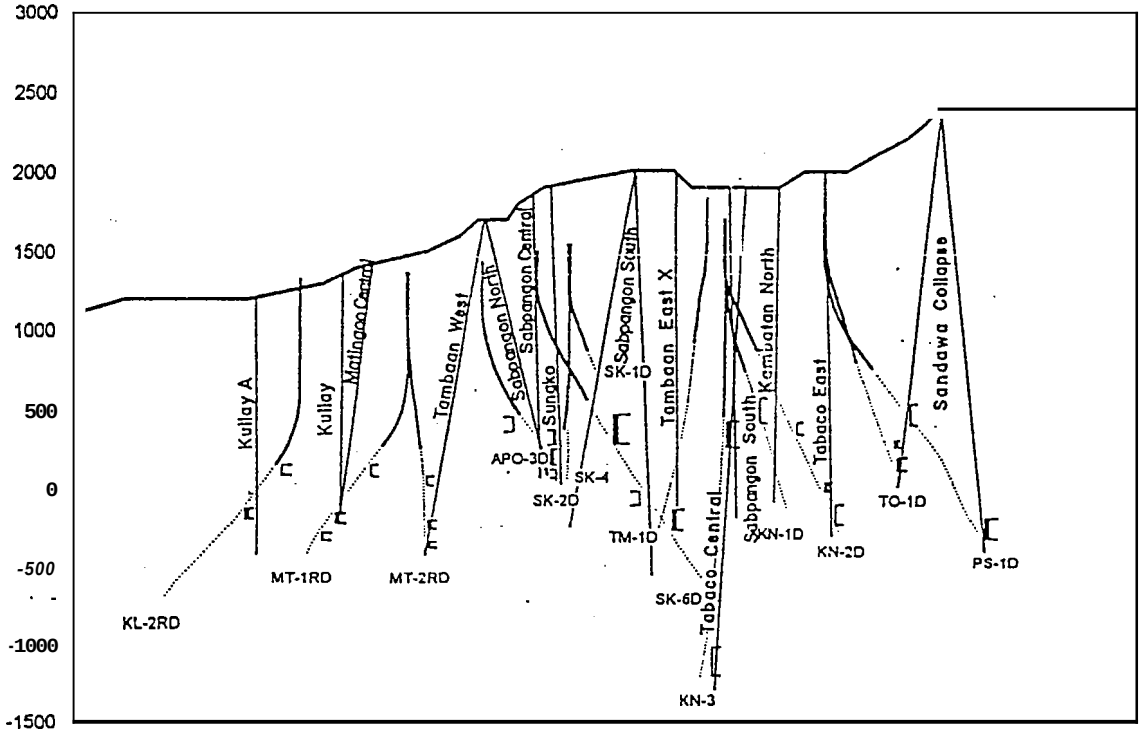

Figure 4. Permeable zones and structural intersects of wells, looking NNE (after PNOC-EDC, 1994).

2.6 BORE OUTPUTS OF THE WELLS

The bore outputs of the production wells are summarised in Table 2. Bore output measurements of wells in the outflow sector deliver liquid enthalpy fluids corresponding to the measured temperature of the major feed zone of the wells. One well discharges near-dry steam fluids from the vapour-dominated zone. Two production wells spudded in the Marbel Corridor is postulated to have tapped the single-phase fluids from the upflow zone beneath the Sandawa Collapse.

Discharge fluids of wells inside the Sandawa Collapse have flowing enthalpies that correspond to two-phase fluid conditions. The two-phase fluids tapped by wells inside the Sandawa Collapse, on the other hand, have discharge enthalpies which range from 1200 to 2300 kJ/kg.

Sector	Wells	Wellhead Pressure *bar g*	Mass Flow *kg/s*	Enthalpy kJ/kg
Marbel Corridor	APO-1D	8.2	71.5	1081
	APO-3D	8.2	64.8	1077
	SP-4D	8.2	78.9	1091
	SK-1D	10.3	20.6	2778
	SK-2D	10.2	38.7	1079
	SK-3D	10.3	38.4	1416
	SK-4	10.2	35.2	1094
	SK-5D	10.5	30.3	1253
	SK-6D	10.3	47.5	1361
Matingao Block	APO-2D	8.0	14.9	1414
	MD-1D	7.6	13.4	1540
Sandawa Collapse	KN-2D	8.0	11.3	1240
	KN-3	8.0	33.4	1886
	TM-1D	8.0	16.2	1354
	TM-2D	8.0	26.8	1753
	TM-3D	8.0	16.3	2225

Table2 Bore output of productions wells at operating wellhead pressure.

2.7 CONCEPTUAL MODEL OF THE FIELD

The upwelling of hot geothermal fluids with temperatures greater than 300°C occurs beneath the Sandawa Collapse. The heat source is postulated to be beneath this sector, near Mt. Apo, and is the driving force of the convective system in the reservoir. A two-phase fluid zone overlies the single-phase fluid and boiling is believed to occur at depths -250 m RSL to 0 m RSL. Boiling causes the formation of a vapour dominated zone overlying the two-pbase zone and parts of the outflow zone (Figure 5).

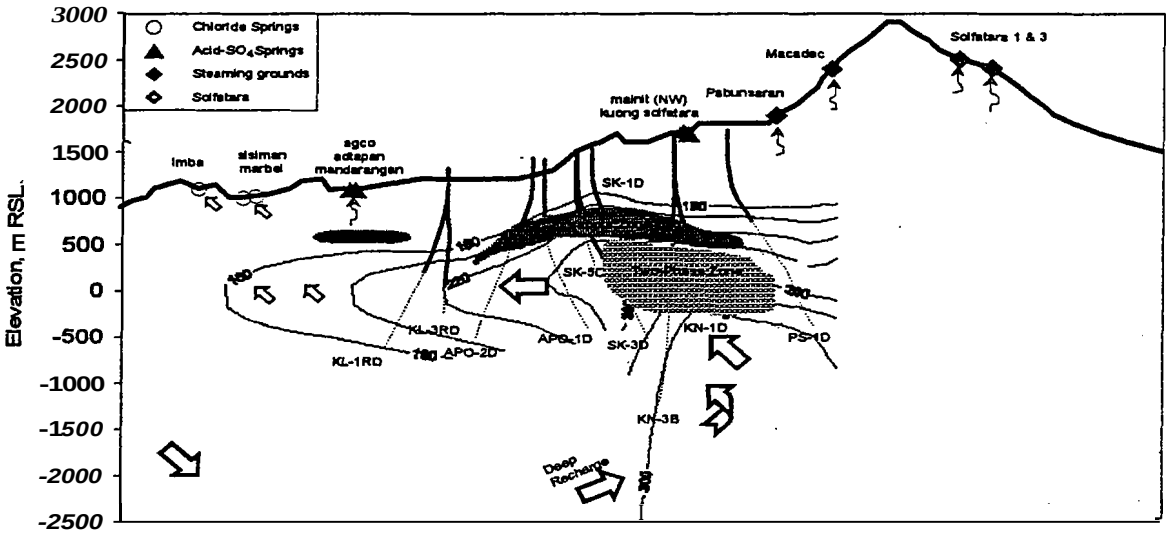

Figure 5. The integrated hydrothermal model of M1GF, looking NNE (modified after Salonga, 1994).

The outflow is towards the northwest where the various NW-SE trending faults in the Marbel Comdor serve as the conduits for the thermal fluids. The outflow is characterised by temperature reversal at depth as observed in the wells drilled in this sector. The flow is then diverted towards the north upon encountering the cold Matingao Block The fluids are then discharged to the surface by the chloride springs of Imba, Marbel and Sisiman.

The topography suggests that recharge comes from the surrounding areas of high elevation. Meteoric waters, together with the descending outflowing fluids, serve as the deep recharge of the system.

3 NATURAL STATE SIMULATION

3.1 The Modelling Process

The main aim of simulating a geothermal system is to set-up a computer model that will best represent the steady state parameters of the real reservoir. The best fit natural state model can then be confidently used to simulate the performance of the field during future large-scale exploitation. The model should encompass the convective system, covering an area larger than the resistivity boundary, and should include enough volume (area and depth). To model the system, a computer model having a number of interconnected blocks is set-up. The structure of the model should be simple to begin with (O'Sullivan and McKibbin, 1989).

The first step in modelling the reservoir is to estimate the permeability of the individual blocks. The initial permeability distribution are based on well test data and on the location of the permeable zones. For

blocks where permeability data are not available, values were inferred from geoscientific data such as structural faults. The initial horizontal permeabilities assigned on the blocks ranged from 1 darcy to 100 darcies, while the vertical permeabilities varied from 0.1 *darcy* to 2 darcies.

The model was run to a *steady* state and the results are then compared with field data. In an attempt to achieve a better match with the field data, permeability values were changed in some blocks.

In the absence of mass flow measurements for chloride springs in M1GF, an initial mass input was assumed at the bottom blocks of the model that corresponds to the postulated upflow zone. The mass input on these blocks represents the mass through-put in the upflow area. The values were varied gradually until a good match between the model results and the stable reservoir parameters were attained.

The MULKOM computer code was used for the numerical modelling at M1GF. It is an integrated finite difference computer code designed to solve heat and mass balance equations. The heat and mass balance fluxes are derived from Darcy's law.

3.2 The Geometry of the Grid-Block System

The numerical model of M1GF covers a total area of 130 km2 encompassing the 30 km2 area defined by the resistivity boundary. The grid-block system consists of fifty-four 1000 m x 1000 m square blocks containing the area covered by the resistivity boundary. Larger grid blocks cover the areas outside the resistivity boundary (Figures *6* and **7).**

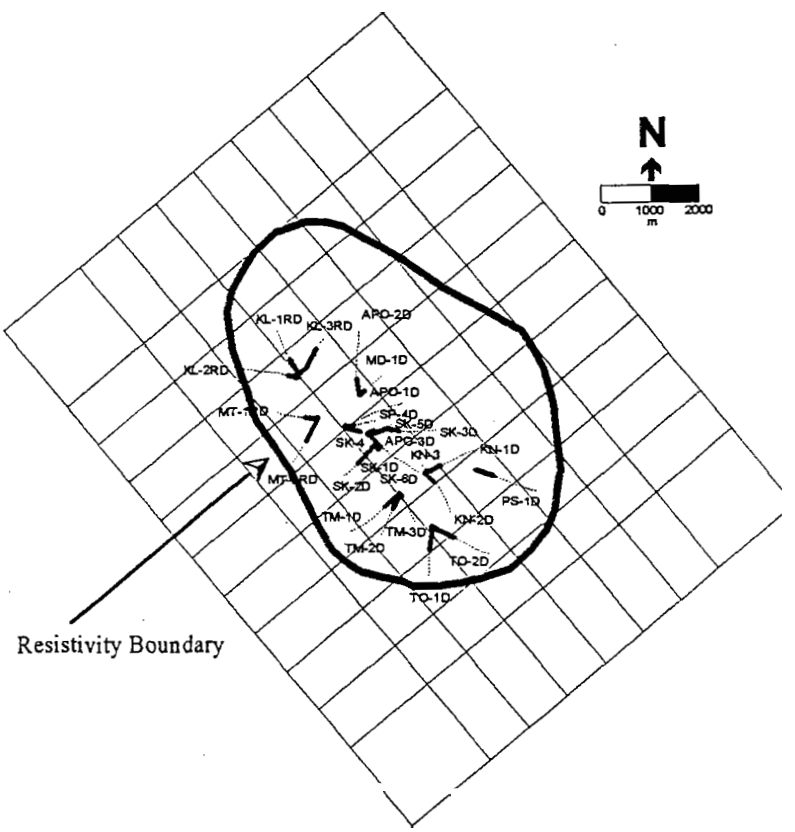

Figure 6. The geometry of the model encompassing the inferred resistivity boundary.

The top surface of each column is meant to match the groundwater table and the thickness vary depending on the inferred groundwater level. Each column extends down to the full depth of the model. It has a total of nine layers with a maximum vertical depth of 3200 m. The base is at -2000 m RSL. No attempt was made to match the layers with individual rock units. The layers are labeled from the top: SS for the surface layer, AA, BB, CC, DD, EE, FF, GG, and HH (Figure 7). There are 880 blocks in the model including the atmosphere blocks above the model's surface. The atmosphere blocks are assumed as fully saturated with groundwater, with initial conditions of 20°C and 101.4 kPa, except the atmospheric blocks above the vapour-dominated blocks where a temperature of 100°C was assumed Blocks HH47, HH48, HH49, HH67, HH68, HH69, HH87, HH88, HH89 served as the recharge blocks in the model

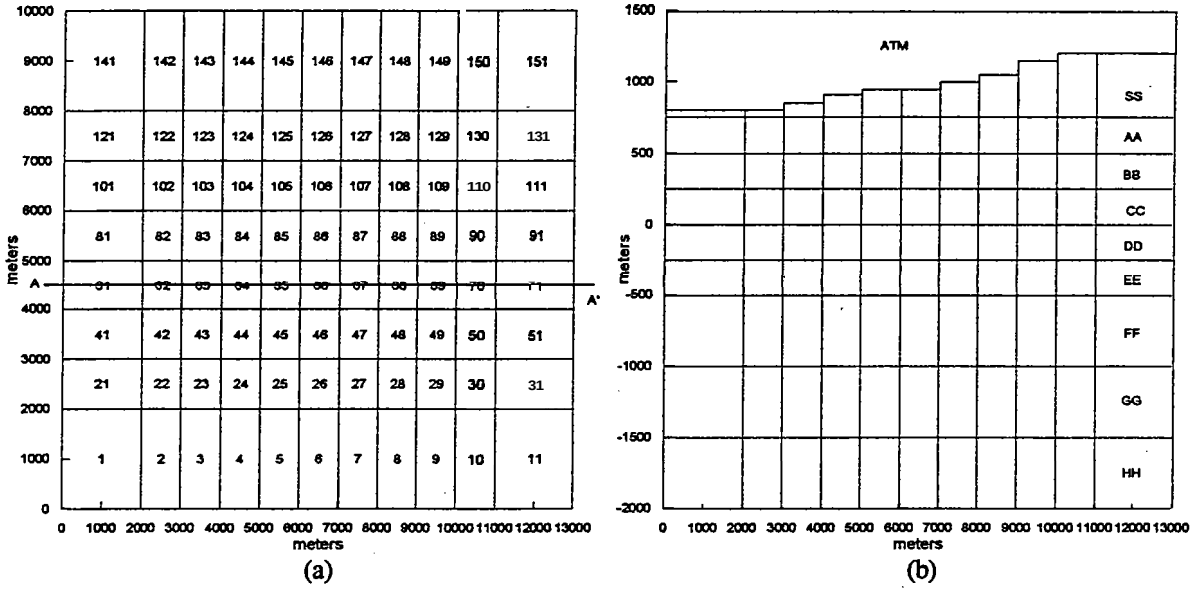

Figure 7. (a) Grid-block system (b) Vertical slice of the system looking along line AA'.

3.3 Best Fit Model

Computer simulation runs were made over a long period of time equivalent to the evolution of the hydrothermal system over geological time. Adjustments of the reservoir parameters were constantly made until a good fit of the measured and calculated temperatures and pressures were attained These parameters were the horizontal and vertical permeabilities and the mass inputs at the bottom blocks of the upflow zone.

The best natural state model configuration was achieved after a total simulated time of 7.6×10^9 years. There were eight materials, based on the physical values, used in the model of varying permeability values. The material properties for the test fit model are given in Table 3 and their distribution in the reservoir (along line AA') is shown in Figure 8. All of the rock types are assumed to have the same values of rock density, heat capacity and porosity. Simulation results show that these storage parameters do not influence the calculated

Material	Density kg/m^3	Heat Capacity $kJ/kg°C$	Thermal Conductivity $W/m°C$	Porosity	Horizontal Permeability $x\ 10^{-15}\ m^2$	Vertical Permeability $x\ 10^{-15}\ m^2$
HIGH	2500	1000	2.5	0.1	80.0	1.0
MED1	2500	1000	2.5	0.1	30.0	1.0
MED2	2500	1000	2.5	0.1	1.0	1.0
LOW1	2500	1000	2.5	0.1	1.0	0.1
LOW2	2500	1000	2.5	0.1	1.0	3.0
LOW3	2500	1000	2.5	0.1	1.0	8.0
SURF	2500	1000	2.5	0.1	0.1	0.2
SUR2	2500	1000	2.5	0.1	0.1	5.0

Table 3. Material properties for the best fit model.

equilibrium temperatures and pressures.

Vertical permeabilities in the upflow zone are 3 to S times higher than in the **outflow** sector. These causes the upwelling of thermal fluids beneath the Sandawa Collapse. Horizontal permeabilities in the outflow sector at **shallow** levels are 30 to SO times greater than in the upflow **zone** causing the fluids to flow towards the Marbel Comdor.

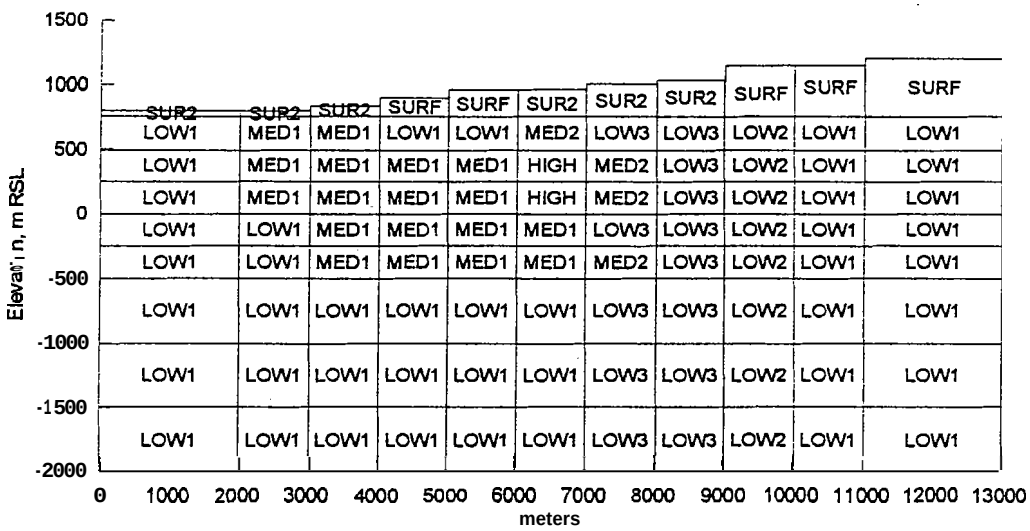

Figure 8. Distribution of the reservoir properties for the **best** model looking along line **AA'.**

Figure 9 show the comparison between the observed and the calculated temperature profiles for the different sectors. There is a good agreement between the observed and calculated temperatures and pressures with depth in **all** sectors **as** illustrated in Figures 9 and 10.

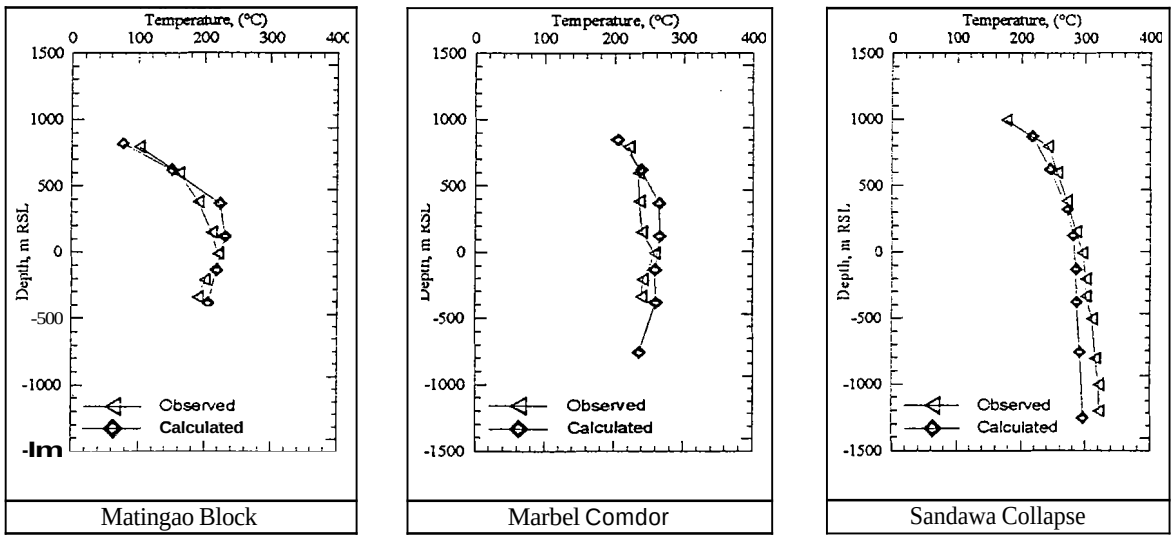

Figure 9. Comparison between the observed and calculated temperature profiles in the different sectors.

Matching the shallow steamdominated zone observed at SK-ID profiles and later at TM-3D discharge was not entirely successful. The calculated vapour saturation values of the shallow blocks were not high enough to duplicate the high steam discharge of SK-1D. Well SK-1D discharge is structurally controlled and the block where the well is situated is relatively large (1 km x 1 km, 250 m depth); thus the calculated average vapour saturation is lower.

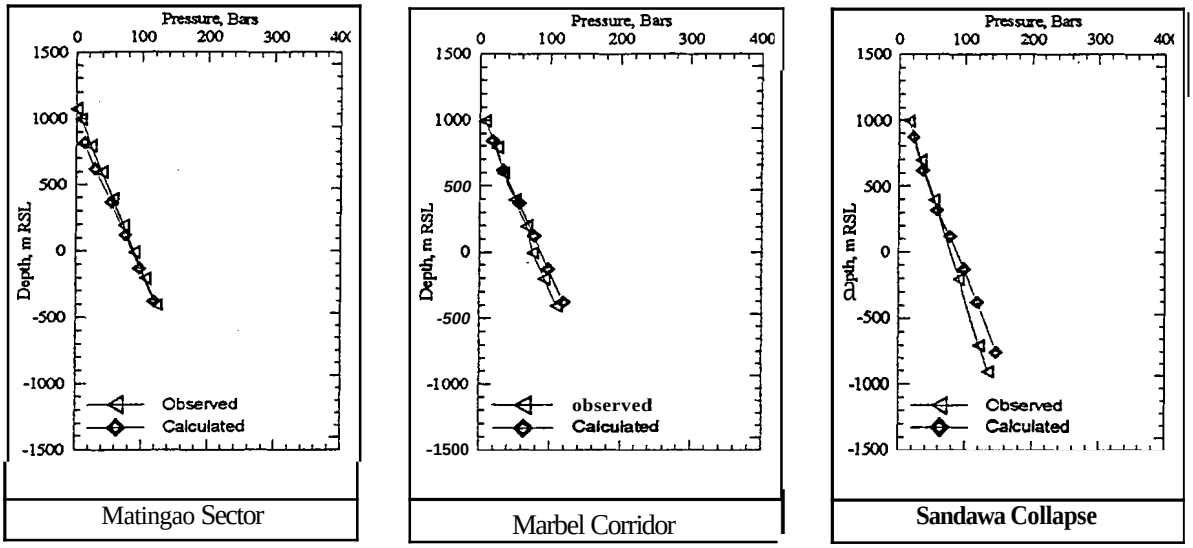

Figure 10. Comparison between the observed and calculated pressure profiles on each sector.

The steady state temperature distribution of the natural state is illustrated in Figure 11. The best natural state model obtained gave good matches to the measured tempertures and pressures. The major features from the conceptual model was closely duplicated by the model. These are the upflowing fluids beneath the Sandawa Collapse, the two-phase zone at shallow levels beneath the Sandawa Collapse, the outflow zone along the Marbel Corridor and the reversal at depths beneath the outflow zone.

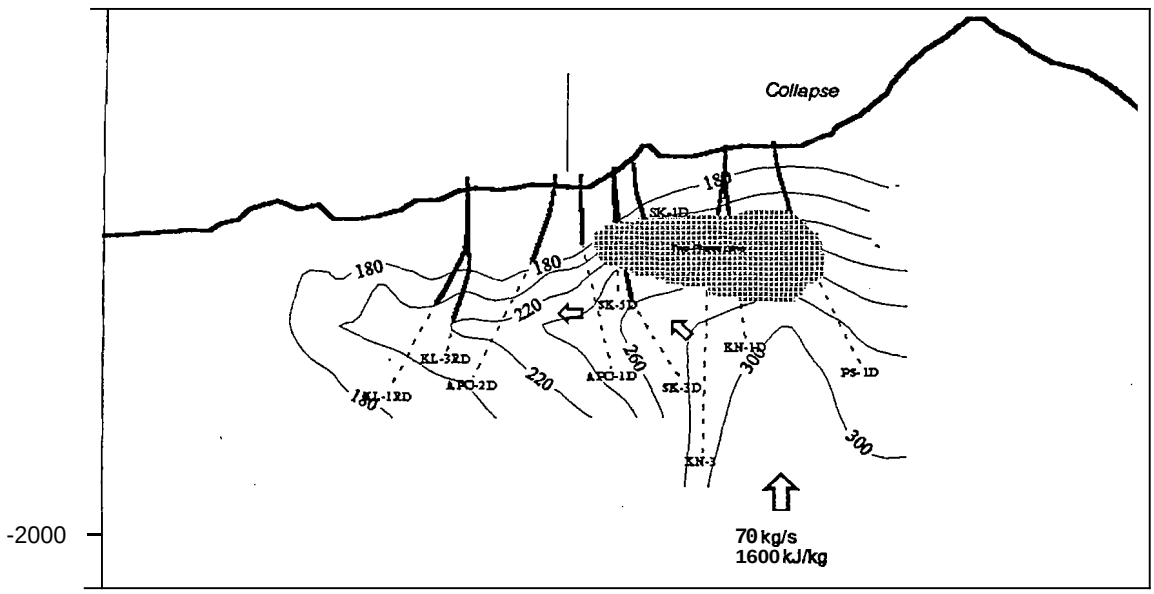

Figure 11. The natural state model of the reservoir, looking along line AA'

4 CONCLUSIONS AND RECOMMENDATIONS

The natural state numerical model of the Mindanao I Geothermal Field was generated using the MULKOM geothermal simulator. The best fit model fairly matches the relevant data and reasonably represented main flowpath features from the conceptual model of the reservoir. The model, however, is not entirely correct considering that the steam-dominated zone was not successfully matched.

The model obtained should be improved by adjusting further the assigned storage parameters. modifying or assigning new rock types that would fit the true natural state, and using a finer grid-block system on zones where it is deemed necessary. The refined model will eventually serve as the basis for developing an exploitation model, where the production data is assimilated into the model.

ACKNOWLEDGEMENTS

I would like to thank Prof Mike J. O'Sullivan for all the help he has extended to me in making this project. Many thanks to Juliet A Newson for her assistance in running the MULKOM simulator and for some helpful tips.

I wish to thank my friends in Apo, Pim Daza, Dave Yglopaz and Noel Salonga for sending the needed data to the Geothermal Institute, to Benson Sambrano and James Nogara in generating some of the figures and to Eric Gonzales for editing this paper.

REFERENCES

O'SULLIVAN, M.J. and McKIBBIN, R. (1989): A Manual for Geothermal Reservoir Engineering Courses at the Geothermal Institute, University of Auckland.

PNOC-EDC. (1989): Mt. Apo Geothermal Project Preliminary Resource Assessment Internal Report.

PNOC-EDC. (1994): Mindanao 1 Geothermal Project, Resource Assessment Update. Internal Report.

SALONGA, N.D. (1995): Fluid and Mineral Equilibria in Acid NaCl (+SO4) Reservoir The Case of Sandawa Collapse, Mt. Apo Hydrothermal System. PNOC-EDC Internal Report.